

CogTree: Cognition Tree Loss for Unbiased Scene Graph Generation

Jing Yu,^{1,3*†} Yuan Chai,^{1,2†} Yue Hu,^{1,3} Qi Wu⁴

¹ Institute of Information Engineering, Chinese Academy of Sciences, Beijing, China

² Intelligent Computing and Machine Learning Lab, School of ASEE, Beihang University, Beijing, China

³ School of Cyber Security, University of Chinese Academy of Sciences, Beijing, China

⁴ University of Adelaide, Australia

{yujing02, huyue}@iie.ac.cn, chaiyuan@buaa.edu.cn, qi.wu01@adelaide.edu.au

Abstract

Scene graphs are semantic abstraction of images that encourage visual understanding and reasoning. However, the performance of Scene Graph Generation (SGG) is unsatisfactory when faced with biased data in real-world scenarios. Conventional debiasing research mainly studies from the view of data representation, e.g. balancing data distribution or learning unbiased models and representations, ignoring the mechanism that how humans accomplish this task. Inspired by the role of the prefrontal cortex (PFC) in hierarchical reasoning, we analyze this problem from a novel cognition perspective: learning a hierarchical cognitive structure of the highly-biased relationships and navigating that hierarchy to locate the classes, making the tail classes receive more attention in a coarse-to-fine mode. To this end, we propose a novel Cognition Tree (CogTree) loss for unbiased SGG. We first build a cognitive structure CogTree to organize the relationships based on the prediction of a biased SGG model. The CogTree distinguishes remarkably different relationships at first and then focuses on a small portion of easily confused ones. Then, we propose a hierarchical loss specially for this cognitive structure, which supports coarse-to-fine distinction for the correct relationships while progressively eliminating the interference of irrelevant ones. The loss is model-independent and can be applied to various SGG models without extra supervision. The proposed CogTree loss consistently boosts the performance of several state-of-the-art models on the Visual Genome benchmark.

1 Introduction

Making abstraction from an image into high-level semantics is one of the most remarkable capabilities of humans. Scene Graph Generation (SGG) (Krishna et al. 2017) – a task of extracting objects and their semantic relationships in an image to form a graphical representation – aims to achieve the abstraction capability and bridge the gap between vision and language. SGG has greatly benefited the down-stream tasks in the domain of question answering (Norcliffe-Brown,

*Corresponding author.

†Equal contribution. This work is done when Yuan Chai is an intern in IIE, CAS.

Copyright © 2021, Association for the Advancement of Artificial Intelligence (www.aaai.org). All rights reserved.

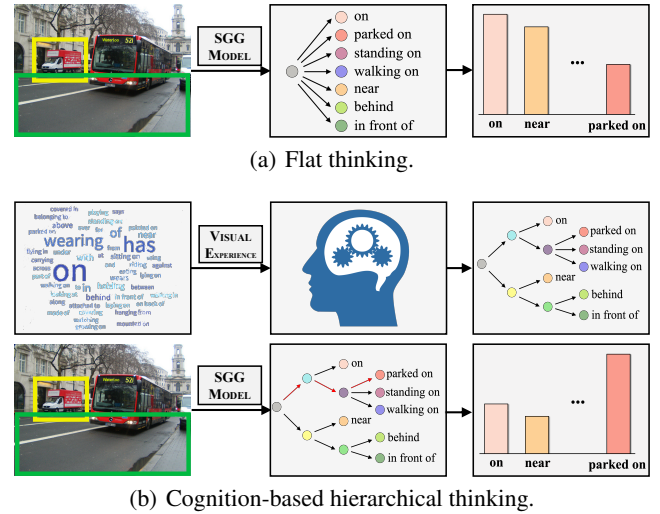


Figure 1: (a) SGG model with conventional flat loss. (b) SGG model with our proposed cognition tree loss. The word size in the top-left box is proportional to the word frequency.

Vafeias, and Parisot 2018; Zhu et al. 2020) and visual understanding (Shi, Zhang, and Li 2019; Jiang et al. 2020). Thereinto, some works (Zhu et al. 2020; Jiang et al. 2020) feed the scene graphs into graph neural networks for relation-aware object representation, and some others (Hudson and Manning 2019) perform sequential reasoning by traversing the relational graphs. Compared with independent objects, the rich relationships in SGG play the predominant role, which improve the performance of down-stream tasks and enable explainable reasoning.

Although much effort has been made in SGG with high accuracy in object detection, most of the detected relationships are far from satisfaction due to the long-tailed data distribution. Only a small portion of the collected relationship classes have abundant samples (head) while most classes contain just a few (tail). This heavily biased training data causes biased relationship prediction. Fine-grained relationships (tail) will be mostly predicted into head classes, which are not accurate or discriminative enough for high-

level reasoning tasks, such as falsely predicting `on` instead of `looking at`, and coarsely predicting `on` instead of `walking on`. Besides, some fine-grained relationships, like `standing on`, `sitting on` and `lying on` can be even harder to distinguish from each other due to their visual similarity and scarce training data.

To tackle this problem, most research focuses on learning unbiased models by re-weighting losses (Zareian, Karaman, and Chang 2020) or disentangling unbiased representations from the biased (Tang et al. 2020). However, humans can effectively infer the correct relationships even when some relationships appear more frequently than others. The essential difference between human and AI systems that has been ignored lies not in the learning strategy or feature representation, but in the way that the concepts are organized. To illustrate this discrepancy, we show an example `trunk parked on street` in Figure 1. Existing models treat all the relationships independently for flat classification (Figure 1(a)). Because of the data bias, the head relationships, *e.g.* `on` and `near`, obtain high predicted probability. In contrast, the recent proposed cognition theory (Sarafyazd and Jazayeri 2019) supports that humans process information hierarchically due to the role of the prefrontal cortex (PFC). In the SGG task, we generally start from making a rough distinction between remarkably different relationships. As shown in Figure 1(b), relationships belonging to the concept “`on`”, *e.g.* `on` and `parked on`, will firstly be distinguished from the ones about “`near`” concept, *e.g.* `near` and `behind`; then we move to distinguish the slight discrepancy among some easily confused ones in one concept, *e.g.* `parked on`, `standing on` and `walking on`, regardless of most irrelevant relationships.

Inspired by the hierarchical reasoning mechanism in PFC, we propose a novel loss function, **Cognition Tree (CogTree)** loss, for unbiased scene graph generation. We first propose to build a hierarchy of the relationships, imitating the knowledge structure built from the independent relationships in human mind. The CogTree is derived from the prediction of a biased SGG model that satisfies the aforementioned thinking principles: distinguishing remarkably different relationships at first and then focusing on a small portion of easily confused ones. Then we design a CogTree-based loss to train the SGG network from scratch. This loss enables the network to surpass the noises from inter-concept relationships and then intra-concept relationships progressively. In this way, the SGG models are no longer required to distinguish each detailed discrepancy among all the relationships as flat thinking, resulting in more accurate prediction due to the coarse-to-fine thinking strategy.

The main contributions are summarized as follows: (1) We exploit the possibility of cognition in SGG by building the cognitive structure of the relationships, which reveals the hierarchy that the relationships are organized after preliminary learning; (2) We propose a hierarchical loss specially for the above cognitive structure, which supports coarse-to-fine distinction for the correct relationships while progressively eliminating the interference of irrelevant ones. It is model-independent and can be applied to various SGG models without extra supervision; (3) We perform extensive eval-

uation on state-of-the-art models and a stronger transformer baseline. Results show that the CogTree loss consistently boosts their performance with remarkable improvement.

2 Related Work

Scene Graph Generation. SGG (Xu et al. 2017) products graphical abstraction of an image and encourages visual relational reasoning and understanding in various downstream tasks (Zhu et al. 2020; Jiang et al. 2020). Early works focus on object detection and relationship detection via independent networks (Lu et al. 2016; Zhang et al. 2017), ignoring the rich contextual information. To incorporate the global visual context, recent works leverage message passing mechanism (Xu et al. 2017; Li et al. 2017; Yang et al. 2018; Li et al. 2018; Qi et al. 2019; Chen et al. 2019a) and recurrent sequential architectures (Zellers et al. 2018; Woo et al. 2018; Tang et al. 2019) for more discriminative object and relationship representations. Although the accuracy is high in object detection, the relationship detection is far from satisfaction due to the heavily biased data. (Chen et al. 2019b; Tang et al. 2019) consider the biased SGG problem and propose mean Recall as the unbiased metric without corresponding debiasing solutions. The recent work (Liang et al. 2019) prunes the predominant spacial relationships and keeps the tail but informative ones in the dataset. (Tang et al. 2020) proposes the first solution for unbiased SGG by counterfactual surgeries on causal graphs. We rethink SGG task from the cognition perspective and novelly solve the bias problem based on the coarse-to-fine structure of the relationships, imitating human’s hierarchical thinking mechanism.

Biased Classification. Classification on highly-biased training data has been extensively studied in previous work, which can be divided into three categories: (1) balancing data distribution by data augmentation or re-sampling (Burnaev, Erofeev, and Papanov 2015; Li, Li, and Vasconcelos 2018; Li and Vasconcelos 2019); (2) debiasing learning strategies by re-weighting losses or training curriculums (Mikolov et al. 2013; Huang et al. 2016; Lin et al. 2017b; Cui et al. 2019); (3) separating biased representations from the unbiased for prediction (Misra et al. 2016; Cadene et al. 2019; Tang et al. 2020). Our CogTree loss belongs to the second category but differs from existing methods in that we first leverage the hierarchical structure inherent in the relationships, which enables more discriminative representation learning by a coarse-to-fine mode.

3 Methodology

The central goal of our CogTree loss is to enable the existing SGG models to generate unbiased scene graphs with highly biased data. Since the CogTree loss is model-independent, in this section, we start by summarizing the framework of conventional biased SGG models. Based on this framework, we propose a novel transformer-based SGG network (SG-Transformer) for better considering contextual information as a stronger baseline. Then we introduce the CogTree building process to adaptively construct the coarse-to-fine structure among the independent relationships from the biased SGG models. A CogTree loss is then proposed to train

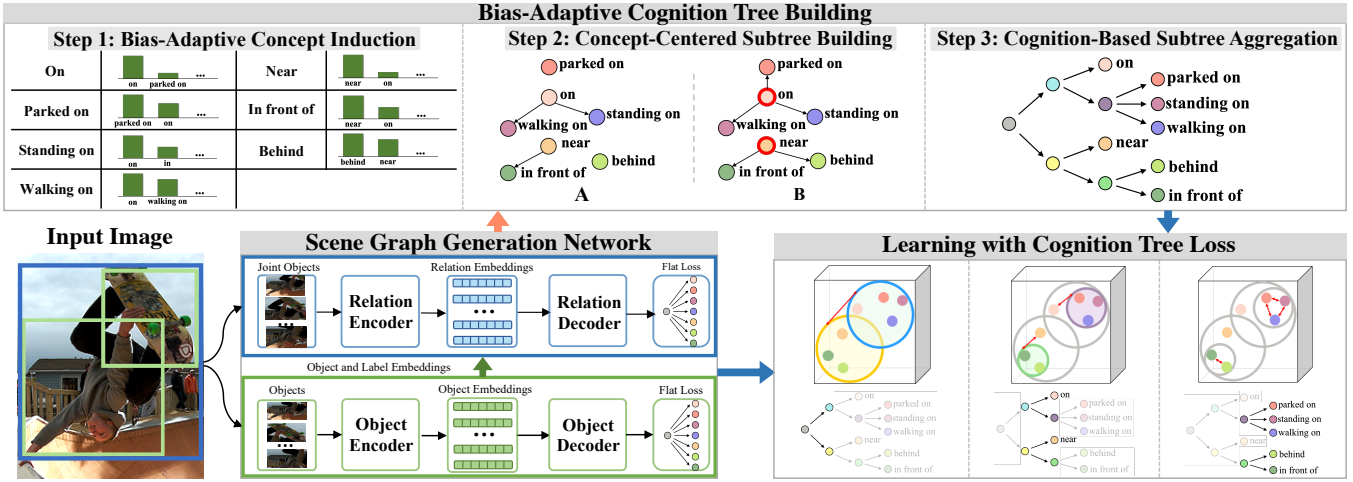


Figure 2: The overview of CogTree loss applied to SGG models. It contains three parts: Scene Graph Generation Network summarizes the framework of biased SGG models; Bias-Adaptive Cognition Tree Building organizes relationships by a coarse-to-fine tree based on biased prediction; Learning with CogTree Loss supports network to distinguish relationships hierarchically.

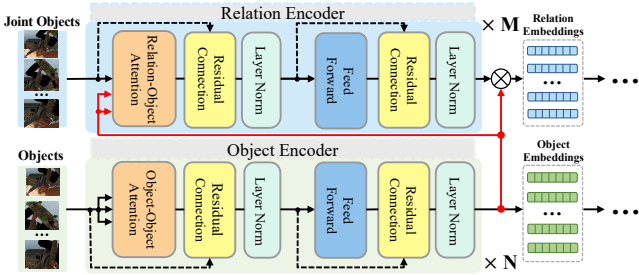


Figure 3: The encoder structure in SG-Transformer.

the network by suppressing inter-concept and intra-concept noises in a hierarchical way, resulting in unbiased scene graphs without requiring extra supervision. The framework is illustrated in Figure 2.

3.1 The Framework of Biased SGG Models

We summarize the SGG framework from three typical models, i.e. the state-of-the-art MOTIFS (Zellers et al. 2018), VCTree (Tang et al. 2019) and our proposed Transformer-based SGG network (SG-Transformer). As shown in Figure 2, it mainly contains two processes: object classification (bottom) and relationship classification (top).

Object classification aims to detect the object locations and object classes in an image. Typically, a pre-trained Faster R-CNN (Ren et al. 2015) is applied to extract K objects $O = \{o_i\}^K$ and describe object o_i by the visual feature v_i , the initial object class probabilities c_i , and the spatial feature b_i . The above three kinds of contextual features are concatenated, linear transformed and fed into $Encoder_o$ to obtain the object embedding m_i , which is then decoded by $Decoder_o$ to predict its fine-tuned object label l_i^o .

It is a beneficial prior that some objects always co-occur in different scenes, which is an informative clue to enrich object semantics. In MOTIFS and VCTree,

LSTMs/TreeLSTMs are used in $Encoder_o$ and $Decoder_o$ to capture the co-occurrence among objects. In this work, we propose a transformer-based $Encoder_o$ to adaptively gather multi-view contextual information for a certain object without the limitation of sequential inputs. As shown in the bottom of Figure 3, the encoder consists of N object-to-object (O2O) blocks and each block contains a multi-head self-attention layer followed by a fully-connected layer, both succeeded with residual connection and layer normalization (Vaswani et al. 2017). Our $Decoder_o$ is a fully connected layer followed by a softmax layer.

Relationship classification predicts the relationship l_{ij}^r between objects o_i and o_j by typically taking three inputs: object embeddings v_i and v_j , word embeddings of the object predictions s_i and s_j , and the visual features of the union region v_{ij} . MOTIFS and VCTree utilize sum fusion as $Encoder_r$ and a fully connected layer as $Decoder_r$.

Unlike previous works that only encode subject and object features, we observe that the global objects are also beneficial for relationship representations. For example, wave, beach and their spatial information will help to distinguish whether the relationship is man-riding-surfboard or man-carrying-surfboard. Therefore, we propose a transformer-based $Encoder_r$ to adaptively capture such contextual semantics by M relation-to-object (R2O) blocks. R2O differs from O2O only in that the self-attention layer is replaced by a cross-attention layer to gather relevant information from global objects $\{m_i\}^K$. The input relationship embedding r_{ij} is computed by a linear transformation of the concatenated feature $[v_{ij}, s_i, s_j, b_i, b_j]$. The output of the last R2O block will be concatenated with subject m_i and object m_j orderly, and fed into the $Decoder_r$, a fully connected layer followed by a softmax layer, to predict l_{ij}^r .

Training loss is the softmax cross-entropy loss (Zellers et al. 2018) for both object and relationship classification. It can be regarded as flat thinking that treats all the classes independently and makes prediction at one time.

3.2 Bias-Adaptive Cognition Tree Building

Once the above SGG models have been trained on the imbalanced data, the biased models are most likely to predict fine-grained relationships (tail) into inaccurate but reasonable head ones. The models can make rough distinction between remarkably different kinds of relationships. Once predicted into the same class, different relationships mostly share similar properties on either visual appearance (e.g. walking on and standing on) or high-level semantics (e.g. has and with). We term each distinct kind of relationships sharing similar properties as a *concept*. Next, we induce concepts from all the relationships and represent their hierarchical structure by a cognition tree. As shown on the top of Figure 2, this process includes the following three steps (see Appendix 1 for the pseudo code):

Step 1: Bias-Adaptive Concept Induction. We first induct each relationship into a certain concept based on the biased predictions. Specifically, for all the samples with the same ground-truth class d_i , we predict their relationships via a biased model and calculate the distribution of predicted label frequency, denoted as P_i . The most frequently predicted class for the ground-truth class d_i is regarded as its *concept relationship*. As shown in Figure 2, *on* is the concept relationship of itself and *standing on*. The above operation induces all the relationships into C concepts with corresponding concept relationships $\{c_i\}^C$.

Step 2: Concept-Centered Subtree Building. We represent the containment structure of relationships in each concept by a *Concept-Centered Subtree*. For the i^{th} subtree, the root is c_i while the leaves are the relationships induced in this concept. Let the edges pointing from the root to the leaves, indicating the containment relations. Note that, if a subtree only contains the root c_j without leaves, e.g. *parked on* in Figure 2, we directly link it to the concept relationship c_k , which has the second highest frequency in P_j and has leaves in its subtree. This operation supports to induce some tail but isolated relationships into the most approximate concepts. This process outputs T subtrees.

Step 3: Cognition-Based Subtree Aggregation. At last, we aggregate all the subtrees into one CogTree by a coarse-to-fine approach: we construct 4 layers, including *root layer* y_0 , *concept layer* y_1 , *coarse-fine layer* y_2 and *fine-grained layer* y_3 , one at a time progressively. The goal of each layer is to induce relationships into coarser groups than the layer that comes after it. As illustrated in Figure 4, y_1 contains T virtual nodes, each representing a subtree induced in Step 2. The following y_2 layer distinguishes the coarse and fine-grained relationships in that subtree by splitting each node in y_1 into two nodes: one leaf node indicating the concept relationship while the other virtual node representing the cluster of fine-grained relationships. It is worth mentioning that y_2 only focuses on distinguishing whether the input can be described by a coarse or fine-grained relationship, without the burden of discriminating slight discrepancy among the fine-grained ones. The virtual node in y_2 links to its fine-grained relationships of this concept in y_3 , which only contains easily confused ones, e.g. *standing on* and *walking on*, regardless of most irrelevant relationships.

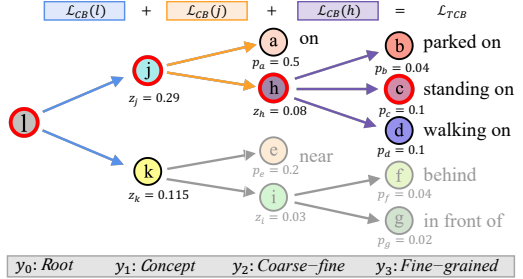


Figure 4: Illustration of calculating the TCB loss.

3.3 Learning with Cognition Tree Loss

Even though the SGG models are encouraged to separate relationships by “flat” cross-entropy loss, it is non-trivial to clearly separate both coarse and fine-grained relationships at one time, especially when similarities existed among them. In fact, it is not a one-shot deal in human mind. Throughout this section, we make unbiased predictions by training the SGG models from scratch based on the above induced CogTree, imitating humans’ hierarchical thinking. The basic idea is illustrated in the bottom right of Figure 2. We add loss terms that further encourage the models to separate relationships from coarse to fine progressively. As shown in Figure 4, we define the loss terms as follows:

Ground-Truth Labels. Given the ground-truth label of a sample, we track the path from the root to the ground-truth leaf node in CogTree and denote the path as $S_0 \rightarrow S_1 \rightarrow \dots \rightarrow S_K$, where the k^{th} node S_k in the path denotes the ground-truth node at layer k . $K=2$ or 3 in our CogTree.

Predicted Probability. Given a sample, the predicted probabilities over all the classes D_r from a biased model is denoted as $P_{pred} = \{p_1, \dots, p_{D_r}\}$. The probability of each leaf node in CogTree corresponds to the value in P_{pred} with the same class. The probability of each internal node is the average value of its children. For the internal node i , we denote z_i as its own probability and $Z(i)$ as the set of probabilities of its children.

Class-Balanced Weight. Since the success of re-weighting strategy for debiasing, we adopt a well performed weighting factor $w_i = (1-\beta)/(1-\beta^{n_i})$ (Cui et al. 2019) as the balance weight of a leaf node, with the hyper-parameter $\beta \in [0, 1]$ and the sample number n_i of the leaf class. For the weight of each internal node, we compute the average value of its children in the same way as probability computation. We denote w_i as the weight of node i .

Cognition Tree Loss. It contains two parts: the class-balanced (CB) softmax cross-entropy loss for “flat” thinking among independent relationships and the tree-based class-balanced (TCB) softmax cross-entropy loss for “coarse-to-fine” thinking along the ground-truth path in CogTree. Given a sample with the ground-truth label d_i , the CB loss is computed between predicted probabilities P_{pred} and label d_i as:

$$\mathcal{L}_{CB} = -w_{d_i} \log\left(\frac{\exp(p_{d_i})}{\sum_{p_j \in P_{pred}} \exp(p_j)}\right) \quad (1)$$

For this sample, if the ground-truth path in CogTree has

Table 1: State-of-the-art comparison on Visual Genome dataset.

Model	Scene Graph Detection			Scene Graph Classification			Predicate Classification		
	mR@20	mR@50	mR@100	mR@20	mR@50	mR@100	mR@20	mR@50	mR@100
IMP+	-	3.8	4.8	-	5.8	6.0	-	9.8	10.5
FREQ	4.5	6.1	7.1	5.1	7.2	8.5	8.3	13.0	16.0
KERN	-	6.4	7.3	-	9.4	10.0	-	17.7	19.2
MOTIFS	4.2	5.7	6.6	6.3	7.7	8.2	10.8	14.0	15.3
VCTree	5.2	6.9	8.0	8.2	10.1	10.8	14.0	17.9	19.4
MOTIFS (baseline)	4.1	5.5	6.8	6.5	8.0	8.5	11.5	14.6	15.8
MOTIFS + Focal	3.9	5.3	6.6	6.3	8.0	8.5	11.5	14.6	15.8
MOTIFS + Reweight	6.5	8.4	9.8	8.4	10.1	10.9	16.0	20.0	21.9
MOTIFS + Resample	5.9	8.2	9.7	9.1	11.0	11.8	14.7	18.5	20.0
MOTIFS + TDE	5.8	8.2	9.8	9.8	13.1	14.9	18.5	25.5	29.1
MOTIFS + CogTree	7.9	10.4	11.8	12.1	14.9	16.1	20.9	26.4	29.0
VCTree (baseline)	4.2	5.7	6.9	6.2	7.5	7.9	11.7	14.9	16.1
VCTree + TDE	6.9	9.3	11.1	8.9	12.2	14.0	18.4	25.4	28.7
VCTree + CogTree	7.8	10.4	12.1	15.4	18.8	19.9	22.0	27.6	29.7
SG-transformer (baseline)	5.6	7.7	9.0	8.6	11.5	12.3	14.4	18.5	20.2
SG-transformer + CogTree	7.9	11.1	12.7	13.0	15.7	16.7	22.9	28.4	31.0

$K + 1$ nodes, except the leaf node, we would have K different terms in our TCB loss. For the root and each internal node in the ground-truth path, we compute the class-balanced softmax cross-entropy across the children and average over all the terms to obtain the TCB loss as:

$$\mathcal{L}_{TCB} = \frac{1}{K} \sum_{k=1}^K -w_{S_k} \log\left(\frac{\exp(z_{S_k})}{\sum_{z_j \in Z(S_{k-1})} \exp(z_j)}\right) \quad (2)$$

TCB loss enables the network to surpass the noises from inter-concept relationships to learn concept-independent representations first, and then surpass the noises from intra-concept relationships to refine relationship-independent representations, resulting in more accurate and discriminative representations. The CogTree loss is defined as a weighted sum of \mathcal{L}_{CB} and \mathcal{L}_{TCB} to leverage both of their advantages:

$$\mathcal{L} = \mathcal{L}_{CB} + \lambda \mathcal{L}_{TCB} \quad (3)$$

where λ is a hyper-parameter. The SGG model is trained from scratch by the CogTree loss without any extra supervision. In the test stage, the models predict via original decoders without any modification.

4 Experiments

Dataset: We evaluate the CogTree loss on the Visual Genome dataset (Krishna et al. 2017), which contains 108k images, 75k object classes and 37k predicate (*i.e.* relationship) classes. Since 92% predicate classes have less than 10 samples, we adopt the widely used VG split (Xu et al. 2017; Zellers et al. 2018; Tang et al. 2019; Chen et al. 2019a; Tang et al. 2020), with the 150 most frequent object classes and 50 predicate classes. The VG split only contains training set and test set and we follow previous work (Zellers et al. 2018) to sample a 5K validation set from the training set.

Tasks and Evaluation: Following previous work (Zellers et al. 2018), the SGG task can be divided into three sub-tasks: (1) Predicate Classification (**PredCls**) takes the

ground-truth object labels and bounding boxes for relationship prediction; (2) Scene Graph Classification (**SGCls**) takes ground-truth bounding boxes for object label prediction; (3) Scene Graph Detection (**SGDet**) predict SGs from scratch. To evaluate the unbiased SGG, we follow (Chen et al. 2019b; Tang et al. 2019) to use the unbiased metric mean Recall@K (**mR@K**), which calculates R@K for each class separately and average R@K for all the classes.

Implementation: We use a pre-trained Faster R-CNN (Ren et al. 2015) with ResNeXt-101-FPN (Lin et al. 2017a) as the object detector. SG-transformer contains 3 O2O blocks, 2 R2O blocks and 12 attention heads. The balanced weight λ in CogTree loss is set to 1. β in the re-weighting factor is set to 0.999. Our models are trained by SGD optimizer with 5 epochs, where the mini-batch size is 12 and the learning rate is 1.2×10^{-3} . All the experiments are implemented with PyTorch and conducted with NVIDIA Tesla V100 GPUs.

4.1 State-of-the-Art Comparison

We evaluate the CogTree loss on three baseline models: MOTIFS, VCTree, and SG-Transformer, and compare the performance with the state-of-the-art debiasing approach TDE (Tang et al. 2020). All the above models share the same pre-trained Faster R-CNN detector and sum fusion decoder (except SG-Transformer). We also compare the performance with existing biased models, including IMP+ (Xu et al. 2017), FREQ (Zellers et al. 2018), KERN (Chen et al. 2019b), MOTIFS (Zellers et al. 2018), and VCTree (Tang et al. 2019, 2020).

In Table 1, we have the following observations: (1) CogTree loss is a stable method that remarkably improves all the baselines on all the metrics. SGcls and Predcls achieve more significant improvements compared with SGDet. (2) CogTree loss consistently outperforms conventional debiasing methods, including focal, reweight and resample, which achieve limited performance increase on MOTIFS. (3) Compared with the state-of-the-art debiasing method TDE, CogTree loss has obvious advantages on all the base-

Table 2: Ablation study of key components in our CogTree loss.

Method	Scene Graph Detection			Scene Graph Classification			Predicate Classification		
	mR@20	mR@50	mR@100	mR@20	mR@50	mR@100	mR@20	mR@50	mR@100
CogTree + \mathcal{L} (full model)	7.92	11.05	12.70	12.96	15.68	16.72	22.89	28.38	30.97
1 CogTree + \mathcal{L}_{TCB}	7.70	10.39	12.07	12.15	15.07	16.15	21.08	27.08	29.41
2 CogTree + \mathcal{L}_{TCE}	7.57	10.53	11.86	12.14	14.42	15.29	21.16	26.14	28.32
3 \mathcal{L}_{CB}	6.74	9.56	11.29	10.76	13.13	13.88	18.02	23.40	25.25
4 \mathcal{L}_{CE}	5.55	7.74	8.98	8.57	11.46	12.27	14.35	18.48	20.21
5 Fuse-layer + \mathcal{L}	5.86	8.02	9.05	8.17	10.39	11.32	13.77	18.87	20.77
6 Fuse-subtree + \mathcal{L}	5.36	7.19	8.28	8.71	10.66	11.61	16.20	20.17	22.12
7 Cluster-tree + \mathcal{L}	5.84	8.10	9.12	8.86	10.88	11.52	15.12	19.20	20.81
8 CogTree + $\mathcal{L}(\text{MAX})$	5.38	7.16	8.16	8.97	10.85	11.83	15.48	19.93	21.87
9 CogTree + $\mathcal{L}(\text{SUM})$	1.86	3.09	3.68	6.58	8.82	9.86	11.31	15.67	17.98



Figure 5: R@100 of the most frequent 35 classes on PredCls.

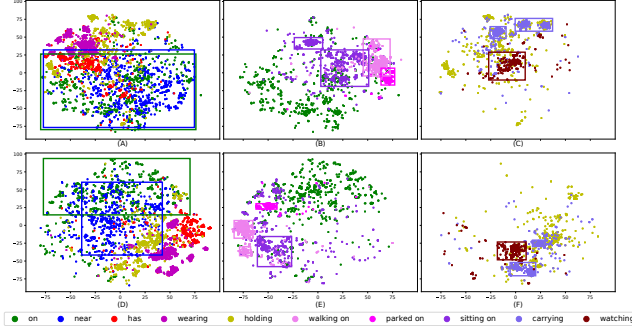


Figure 6: t-SNE visualization of relationship embeddings. A-C are from SG-Transformer while D-F are from SG-Transformer+CogTree.

lines. Moreover, the results of R@K in Appendix 2.1 show a performance increase from TDE to CogTree, which indicates that our method generates better unbiased SGs while keeping more correct head predicates compared with TDE. (4) SG-Transformer consistently outperforms all the existing SGG models and baselines, which verifies that the contextual information gathered by transformer structure is of great benefit for discriminative object and relationship representations. Notably, SG-Transformer achieves new state-of-the-art performance on SGG tasks among the biased models.

We also report the R@100 performance of each class in Figure 5. SG-Transformer+CogTree obviously improves from SG-Transformer at most tail classes but drops from SG-Transformer at a few head classes, further indicating that the increase on mR@K is mainly due to the improvement of the tail classes instead of the head. All the improvement should owe to the discriminative relationship representations leaned by the CogTree loss. As the t-SNE visualiza-

tion shown in Figure 6, samples of different relationships, including both the concept relationships (A, D) and the fine-grained ones (B, C, E, F) are separated more obviously while samples of each relationship are clustered more densely.

4.2 Ablation Study

In Table 2, we show ablation results to verify the contribution of each component in our CogTree loss on the SG-Transformer baseline. In models ‘1-4’, we assess the **effectiveness of each part in the loss**. Compared with the full model, the performance of both ‘1’ and ‘3’ decreases when removing the other loss term, which indicates that both hierarchical and flat losses are beneficial to provide complementary information for SGG tasks. Thereinto, the hierarchical loss has greater influence than the flat one. When removing the class-balanced weight from both ‘1’ and ‘3’, ‘2’ and ‘4’ result in a further decrease. It proves the benefits of re-weighting in model debiasing, though it is obviously less influential on the hierarchical loss. Model ‘4’ utilizes the softmax cross-entropy loss and obtains the worst performance.

In models ‘5-7’, we evaluate the **influence of the tree structure** on the performance (see Appendix 3 for tree structure visualization). The CogTree is built based on two principles: a) Relationships belonging to the same concept are organized in one subtree; b) Relationships in one subtree are organized in different layers from coarse to fine. We manually adjust the induced tree that violates the above principles and evaluate the performance with the same loss \mathcal{L} . In ‘5’, we violate the second principle and place the fine-grained relationships in the same coarse-fine layer as the concept relationship. In ‘6’, we disregard the first principle and mix relationships belonging to different concepts in one subtree. Specifically, we simply link all the concept relationships flatly to the root while placing all the fine-grained relationships flatly in a subtree linked to the root. We can observe a significant decrease in performance when the tree structure does not satisfy either of the two principles. In ‘7’, we build the tree structure by the conventional hierarchical clustering on relationship representations extracted from the last fully-connected layer weights (Wan et al. 2020). This tree is indicative of the visual similarity of relationships, which results in an obvious decrease compared to the full model. It indicates that the relationship hierarchy is better based on semantic correlation instead of visual similarity.

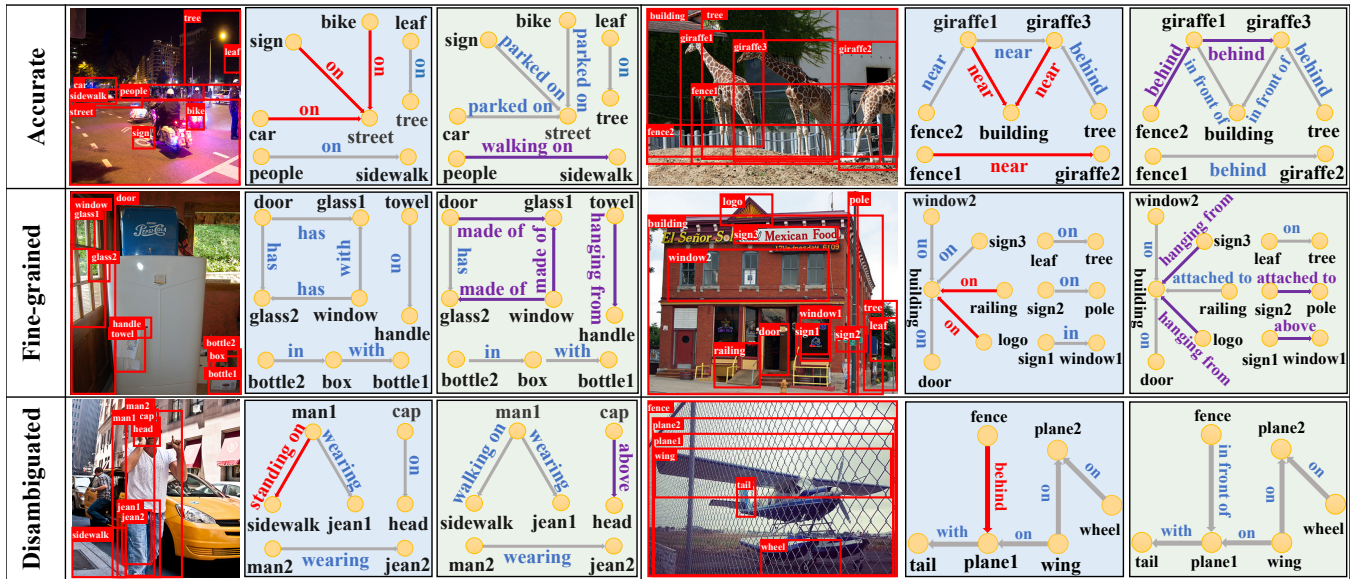


Figure 7: Visualization of scene graphs generated by SG-Transformer (blue) and SG-Transformer+CogTree (green). Compared with the ground-truth, the quality of predicted relationships are marked in three colors: red (false), blue (correct), purple (better).

In models ‘8’ and ‘9’, we test the **influence of different functions: MAX and SUM, for calculating the predicted probabilities and the class-balanced weights** of internal nodes. Compared with the full model using AVERAGE, both ‘8’ and ‘9’ have an obvious performance drop. Further analysis implies that both MAX and SUM increase the predicted probabilities of the internal node in the coarse-fine layer, thus decreasing the incorrect prediction penalty of fine-grained relationships in Eq. 2. In comparison, the increased values of balancing weights by MAX and SUM have less influence on the final performance.

4.3 Qualitative Analysis

We visualize several PredCls samples that generated by SG-Transformer (blue) and SG-Transformer+CogTree (green) in Figure 7. Even though SG-Transformer is the strongest baseline among the three, it still achieves remarkable improvement when equipped with the CogTree loss: (1) CogTree loss encourages the model to predict more accurate and discriminative relationships compared with the baseline. As shown in the first two rows, the baseline prefers to predict the reasonable but trivial head classes `on` and `near` due to the biased training, while our model precisely predicts the fine-grained and informative relationships like `parked on` and `in front of`. It mainly because that the CogTree loss effectively separates the concept relationships apart from the fine-grained ones in the coarse-fine layer. (2) CogTree loss enables the model to distinguish visually and semantically similar relationships, which is quite difficult for the baseline as shown in the last row. The baseline falsely predicts `walking on` as `standing on` since it can not capture the detailed difference between the two actions. Our model succeeds in such prediction by surpassing noises from all the irrelevant relationships and just

Table 3: Performance with different balancing weights.

λ	Scene Graph Detection			Scene Graph Classification			Predicate Classification		
	mR@20	mR@50	mR@100	mR@20	mR@50	mR@100	mR@20	mR@50	mR@100
0.4	7.22	9.72	11.30	12.09	15.03	16.12	21.17	27.20	29.59
0.7	8.62	11.30	12.70	12.22	14.91	15.88	21.28	26.39	28.69
1	7.92	11.05	12.70	12.96	15.68	16.72	22.89	28.38	30.97
1.3	7.84	10.48	12.19	12.35	15.04	15.87	22.06	27.11	29.21
1.6	6.78	9.04	10.22	12.20	14.70	15.82	21.34	26.80	29.18

focusing on semantically similar ones.

4.4 Parameter Analysis

In Table 3, we assess the influence of different values of λ on the performance. $\lambda = 1$ achieves the best performance on most metrics. The performance drops slightly in the range of $[0.7, 1.3]$. We also vary the number of O2O and R2O blocks from 2 to 4 in SG-Transformer (see Appendix 2.2) and obtain the highest mR@K with 3 O2O blocks and 2 R2O blocks. We use the above settings in our full model.

5 Conclusion

In this paper, we propose a CogTree loss to generate unbiased scene graphs with highly biased data, which focuses on hierarchical relationship distinction from the cognition perspective. We novelly leverage the biased prediction from SGG models to organize the independent relationships by a tree structure, which contains multiple layers corresponding to the relationships from coarse to fine. We propose a CogTree loss specially for the above tree structure that supports hierarchical distinction for the correct relationships while progressively eliminating the irrelevant ones. The loss is model-independent and consistently boosting the performance of various SGG models with remarkable improvement. How to incorporate commonsense knowledge to optimize the CogTree structure will be our future work.

References

Burnaev, E.; Erofeev, P.; and Papanov, A. 2015. Influence of resampling on accuracy of imbalanced classification. In *ICMV*, 987521–987521.

Cadene, R.; Dancette, C.; Ben younes, H.; Cord, M.; and Parikh, D. 2019. Rubi: reducing unimodal biases for visual question answering. In *NeurIPS*, 841–852.

Chen, L.; Zhang, H.; Xiao, J.; He, X.; Pu, S.; and Chang, S.-F. 2019a. Counterfactual critic multi-agent training for scene graph generation. In *ICCV*, 4613–4623.

Chen, T.; Yu, W.; Chen, R.; and Lin, L. 2019b. Knowledge-embedded routing network for scene graph generation. In *CVPR*, 6163–6171.

Cui, Y.; Jia, M.; Lin, T.-Y.; Song, Y.; and Belongie, S. 2019. Class-balanced loss based on effective number of samples. In *CVPR*, 9268–9277.

Huang, C.; Li, Y.; Change Loy, C.; and Tang, X. 2016. Learning deep representation for imbalanced classification. In *CVPR*, 5375–5384.

Hudson, D.; and Manning, C. D. 2019. Learning by abstraction: the neural state machine. In *NeurIPS*, 5903–5916.

Jiang, X.; Yu, J.; Qin, Z.; Zhuang, Y.; Zhang, X.; Hu, Y.; and Qi, W. 2020. DualVD: an adaptive dual encoding model for deep visual understanding in visual dialogue. In *AAAI*, 11125–11132.

Krishna, R.; Zhu, Y.; Groth, O.; Johnson, J.; Hata, K.; Kravitz, J.; Chen, S.; Kalantidis, Y.; Li, L.-J.; Shamma, D. A.; Bernstein, M. S.; and Fei-Fei, L. 2017. Visual genome: connecting language and vision using crowd-sourced dense image annotations. *IJCV* 123: 32–73.

Li, Y.; Li, Y.; and Vasconcelos, N. 2018. RESOUND: towards action recognition without representation bias. In *ECCV*, 513–528.

Li, Y.; Ouyang, W.; Zhou, B.; Shi, J.; Zhang, C.; and Wang, X. 2018. Factorizable net: an efficient subgraph-based framework for scene graph generation. In *ECCV*, 335–351.

Li, Y.; Ouyang, W.; Zhou, B.; Wang, K.; and Wang, X. 2017. Scene graph generation from objects, phrases and region captions. In *ICCV*, 1261–1270.

Li, Y.; and Vasconcelos, N. 2019. Repair: removing representation bias by dataset resampling. In *CVPR*, 9572–9581.

Liang, Y.; Bai, Y.; Zhang, W.; Qian, X.; Zhu, L.; and Mei, T. 2019. VrR-VG: refocusing visually-relevant relationships. In *ICCV*, 10403–10412.

Lin, T.-Y.; Dollar, P.; Girshick, R.; He, K.; Hariharan, B.; and Belongie, S. 2017a. Feature Pyramid Networks for Object Detection. In *CVPR*, 2117–2125.

Lin, T.-Y.; Goyal, P.; Girshick, R.; He, K.; and Dollár, P. 2017b. Focal loss for dense object detection. In *ICCV*, 2980–2988.

Lu, C.; Krishna, R.; Bernstein, M.; and Fei-Fei, L. 2016. Visual relationship detection with language priors. In *ECCV*, 852–869.

Mikolov, T.; Sutskever, I.; Chen, K.; Corrado, G. S.; and Dean, J. 2013. Distributed representations of words and phrases and their compositionality. In *NeurIPS*, 3111–3119.

Misra, I.; Lawrence Zitnick, C.; Mitchell, M.; and Girshick, R. 2016. Seeing through the human reporting bias: visual classifiers from noisy human-centric labels. In *CVPR*, 2930–2939.

Norcliffe-Brown, W.; Vafeias, S.; and Parisot, S. 2018. Learning conditioned graph structures for interpretable visual question answering. In *NeurIPS*, 8334–8343.

Qi, M.; Li, W.; Yang, Z.; Wang, Y.; and Luo, J. 2019. Attentive relational networks for mapping images to scene graphs. In *CVPR*, 3957–3966.

Ren, S.; He, K.; Girshick, R.; and Sun, J. 2015. Faster R-CNN: towards real-time object detection with region proposal networks. In *NeurIPS*, 91–99.

Sarafyazd, M.; and Jazayeri, M. 2019. Hierarchical reasoning by neural circuits in the frontal cortex. *Science* 364(6441): eaav8911.

Shi, J.; Zhang, H.; and Li, J. 2019. Explainable and explicit visual reasoning over scene graphs. In *CVPR*, 8376–8384.

Tang, K.; Niu, Y.; Huang, J.; Shi, J.; and Zhang, H. 2020. Unbiased scene graph generation from biased training. In *CVPR*, 3716–3725.

Tang, K.; Zhang, H.; Wu, B.; Luo, W.; and Liu, W. 2019. Learning to compose dynamic tree structures for visual contexts. In *CVPR*, 6619–6628.

Vaswani, A.; Shazeer, N.; Parmar, N.; Uszkoreit, J.; Jones, L.; Gomez, A. N.; Kaiser, Ł.; and Polosukhin, I. 2017. Attention is all you need. In *NeurIPS*, 5998–6008.

Wan, A.; Dunlap, L.; Ho, D.; Yin, J.; Lee, S.; Jin, H.; Petryk, S.; Bargal, S. A.; and Gonzalez, J. E. 2020. NBDT: neural-backed decision trees. *arXiv:2004.00221*.

Woo, S.; Kim, D.; Cho, D.; and Kweon, I. S. 2018. Linknet: Relational embedding for scene graph. In *NeurIPS*, 560–570.

Xu, D.; Zhu, Y.; Choy, C. B.; and Fei-Fei, L. 2017. Scene graph generation by iterative message passing. In *CVPR*, 5410–5419.

Yang, J.; Lu, J.; Lee, S.; Batra, D.; and Parikh, D. 2018. Graph r-cnn for scene graph generation. In *ECCV*, 670–685.

Zareian, A.; Karaman, S.; and Chang, S.-F. 2020. Bridging knowledge graphs to generate scene graphs. In *ECCV*.

Zellers, R.; Yatskar, M.; Thomson, S.; and Choi, Y. 2018. Neural Motifs: scene graph parsing with global context. In *CVPR*, 5831–5840.

Zhang, J.; Elhoseiny, M.; Cohen, S.; Chang, W.; and Elgammal, A. 2017. Relationship proposal networks. In *CVPR*, 5678–5686.

Zhu, Z.; Yu, J.; Wang, Y.; Sun, Y.; Hu, Y.; and Wu, Q. 2020. Mucko: multi-Layer cross-modal knowledge reasoning for fact-based visual question answering. In *IJCAI*, 1097–1103.